Crystal Structures of Human Δ4-3-Ketosteroid 5β-Reductase (AKR1D1) Reveal the Presence of an Alternative Binding Site Responsible for Substrate Inhibition[†,‡]

Frédérick Faucher,[§] Line Cantin, Van Luu-The, Fernand Labrie, and Rock Breton*

Oncology and Molecular Endocrinology Research Center, Laval University Medical Center (CHUL) and Laval University, Laval, Québec (QC) G1V 4G2, Canada

Received July 7, 2008; Revised Manuscript Received October 9, 2008

ABSTRACT: The 5β-reductases (AKR1D1−3) are unique enzymes able to catalyze efficiently and in a stereospecific manner the 5β-reduction of the C4−C5 double bond found in Δ4-3-ketosteroids, including steroid hormones and bile acids precursors such as 7α-hydroxy-4-cholesten-3-one and 7α,12α-dihydroxy-4-cholesten-3-one. In order to elucidate the binding mode and substrate specificity in detail, biochemical and structural studies on human 5β-reductase (h5β-red; AKR1D1) have been recently undertaken. The crystal structure of a h5β-red binary complex provides a complete picture of the NADPH−enzyme interactions involving the flexible loop B, which contributes to the maintenance of the cofactor in its binding site by acting as a "safety belt". Structural comparison with binary complexes of AKR1C enzymes, specifically the human type 3 3α-hydroxysteroid dehydrogenase (AKR1C2) and the mouse 17α-hydroxysteroid dehydrogenase (AKR1C21), also revealed particularities in loop B positioning that make the steroid-binding cavity of h5β-red substantially larger than those of the two other enzymes. Kinetic characterization of the purified recombinant h5β-red has shown that this enzyme exerts a strong activity toward progesterone (Prog) and androstenedione (Δ4) but is rapidly inhibited by these substrates once their concentrations reach 2-times their K_m value. A crystal structure of the h5β-red in ternary complex with NADPH and Δ4 has revealed that the large steroid-binding site of this enzyme also contains a subsite in which the Δ4 molecule is found. When bound in this subsite, Δ4 completely impedes the passage of another substrate molecule toward the catalytic site. The importance of this alternative binding site for the inhibition of h5β-red was finally proven by site-directed mutagenesis, which demonstrated that the replacement of one of the residues delineating this site (Val_{309}) by a phenylalanine completely abolishes the substrate inhibition. The results of this report provide structural insights into the substrate inhibition of h5β-red by C19- and C21-steroids.

The 5β-reductase (h5β-red)[1] is known to play a major role in the formation of the cholic and chenodeoxycholic biliary acids (*1*−*3*). More precisely, this enzyme catalyzes the reduction of the bile acid precursors 7α-hydroxycholest-4-en-3-one and 7α,12α-dihydroxycholest-4-en-3-one, to their corresponding 5β-reduced derivatives. Defects in the 5β-red gene result in high urinary and plasma levels of Δ4-3-oxo steroids, which lead to liver failure and hemochromatosis, conditions that are potentially lethal in newborn infants (*4*−*6*).

This enzyme is also important for metabolism of steroid hormones since it efficiently catalyzes the transformation of C21- and C19-steroids and, to a lesser extent, C27-steroids (*7, 8*). Because certain 5β-reduced steroids are active molecules and are possibly involved in many physiological functions (*9*−*13*), the activity of this enzyme is of primary importance. For example, 5β-pregnan-3,20-dione (5β-DHP), the product of the 5β-reduction of progesterone (Prog), is an endogenous ligand for the pregnane X receptor and for the constitutive androstane receptor, both implicated in clearance of xenobiotics (*14*). This Prog metabolite is also a potent tocolytic steroid (*15*) circulating concentrations of which have been found to decrease significantly in the active phase of the first stage of human labor (*16*). Because the relative abundance of 5β-red mRNA in placenta and myometrium also decreases significantly in association with labor (*16*), it has been hypothesized that this enzyme, through the formation of 5β-reduced Prog metabolites, could play a role in regulating myometrial activity and in onset of spontaneous labor in humans.

Contradictory results have however been obtained by different investigators concerning the substrate specificity of

[†] This work was supported by Endorecherche Inc. F.F. is the recipient of a doctoral scholarship provided by the Fonds de la recherche en santé du Québec (FRSQ).

[‡] Atomic coordinates have been deposited with the RCSB Protein Data Bank and are available under the following accession codes: 3CAQ for h5β-reductase/NADPH binary complex and 3CAS h5β-reductase/NADPH/D4 substrate inhibition complex.

* Corresponding author. Mailing address: Centre de Recherche en Endocrinologie Moléculaire et Oncologique, Centre Hospitalier de l'Université Laval (CHUL), 2705 boul. Laurier, Québec (Qc) G1V 4G2, Canada. Tel: (418) 654-2296. Fax: (418) 654-2761. E-mail: rock.breton@crchul.ulaval.ca.

[§] Present address: Department of Microbiology and Molecular Genetics, University of Vermont, Burlington, VT 05405.

[1] Abbreviations: Δ4, androstenedione; h5β-red, human 5β-reductase; h3α-HSD3, human type 3 3α-hydroxysteroid dehydrogenase; 5β-DHP, 5β-pregnan-3,20-dione; AKR, aldo−keto reductases; Prog, progesterone; HSD, hydroxysteroid dehydrogenase; MPD, 2-methyl-2,4-pentanediol; SDR, short-chain dehydrogenase/reductase; Testo, testosterone.

10.1021/bi801276h CCC: $40.75
Published on Web 11/26/2008

Table 1: Dissociation Constant (K_d) of NADPH for Some AKR Enzymes

enzyme	K_d (nM)
h3α-HSD3	2702 ± 140
h5β-reductase	528 ± 28
m17α-HSD	459 ± 24

human 5β-red. Indeed, it was first demonstrated that h5β-red expressed in transiently transfected COS cells showed a small but significant 5β-reduction activity toward cortisol and testosterone (Testo), whereas no activity was detected toward Prog or androstenedione (Δ4) (*17*). It was later found that the same enzyme stably expressed in HEK293 cells catalyzed with similar efficiency the 5β-reduction of Prog, Δ4, and Testo (*7*). These authors also found that cortisol was a poorer substrate for h5β-red, being transformed into its 5β-reduced metabolite at an approximately 20-fold lower rate than Prog. The difference in the experimental conditions used by the two groups (assay of the 5β-red activity in cell homogenates vs intact cells) was then used to explain these contradictory results (*7*). Complementary experiments, especially enzymatic characterization of the purified enzyme, thus seem necessary to better define the steroid substrate specificity of h5β-red.

Human 5β-red belongs to the aldo−keto reductase (AKR) superfamily and is the first member of the 1D subfamily (AKR1D1), which also encompasses the 5β-reductases from rat (AKR1D2) (*18*) and rabbit (AKR1D3). Currently, AKR1D1 encodes the only known human enzyme capable of efficiently catalyzing the 5β-reduction of Δ4-3-ketosteroids. It is highly expressed in the liver (*17*) and, at lower levels, in testes and placenta (*16, 19*). Enzymes of the AKR1D subfamily differ from members of the AKR1C subfamily by the identity of residues forming their catalytic tetrad. Indeed, the His_{117} residue found in the catalytic tetrad of all AKR1C members (Asp_{50}, Tyr_{55}, Lys_{84}, and His_{117}) is substituted by a negatively charged amino acid residue (Glu_{120}) in the AKR1D sequences (Asp_{53}, Tyr_{58}, Lys_{87}, and Glu_{120}). To further refine the catalytic role played by the Glu_{120} residue in the specificity of the 5β-reductase, we have initiated crystallographic studies on the human enzyme (AKR1D1). Very recently, we have determined the first structure for h5β-red in ternary complex with $NADP^+$ and 5β-dihydroprogesterone (*20*) and found that Glu_{120} is not directly involved in catalysis, as previously hypothesized (*21*), but may instead be important for the proper positioning of the steroid substrate in the catalytic site.

Using our homogeneous and highly active enzyme preparation, we decided to more completely characterize the enzymatic activity of h5β-red toward steroid substrates. We thus noted that this enzyme is strongly inhibited by the steroids Δ4 and Prog at concentrations that do not exceed 2-times their K_m value. It has been previously reported that h5β-red can be strongly reduced or inhibited by mineralocorticoids, especially cortisol (*22*). However, the mechanism by which cortisol affects h5β-red activity is currently unknown, as is the capacity of the other steroid hormones to inhibit this enzyme. To better understand, at a molecular level, the mechanism underlying the substrate inhibition, we also performed structural characterization of this enzyme, in two different complexes: a binary complex with NADPH and a ternary complex with cofactor and Δ4. The position and orientation of Δ4 bound inside the steroid-binding site of the h5β-red gave us crucial information on the mechanism by which steroids can influence the activity of this enzyme.

MATERIAL AND METHODS

Recombinant Human 5β-Reductase Expression and Purification. h5β-Reductase was expressed and purified as described previously (*20*). Briefly, a GST−h5β-red fusion protein was expressed in *E. coli*. The expressed fusion protein was then purified and cleaved using successively a gluthatione−sepharose column, anion exchange, and gel filtration. The highly purified protein was finally concentrated to 10−12 mg/mL in a solution containing 10 mM Tris (pH 8.0) and 1 mM β-mercaptoethanol and stored at 4 °C.

Steady-State Enzyme Kinetics. Determination of kinetic constants for Δ4 reduction was performed as described previously (*23, 24*). Briefly, the reactions were performed for 15−60 min at 37 °C using a homogeneous preparation of h5β-red enzyme (0.03−0.1 μM/assay) in a final volume of 800 μL in PBS buffer (140 mM NaCl, 2.7 mM KCl, 10 mM Na_2HPO_4, 1.8 mM KH_2PO_4, pH 7.3) containing 0.5 mM NADPH, 0.1 μM ^{14}C-labeled steroid, and various concentrations of unlabeled steroid. Each velocity measurement was performed using a five-point curve in duplicate. After incubation, the steroids were extracted twice with 1 mL of ether, then resuspended in 40 μL of CH_2Cl_2 and subjected to silica gel 60 thin layer chromatography (MERCK), before separation by migration in the $CHCl_3$/ether (10:3 v/v) solvent system. Substrate and metabolites were revealed by autoradiography and identified by comparison with reference steroids. Kinetic parameters were calculated using the GraphPad Prism 4 program using the Michaelis−Menten equation. When substrate inhibition was detected, an equation for substrate inhibition ($Y = (V_{max}S + V_i(S^2/K_i))/(K_m + S + S^2/K_i)$) was instead used.

Determination of Binding Constant for NADPH by Fluorescence Titration. Fluorescence titration assays were conducted essentially as previously described (*23*). Briefly, the binding constant (K_d) of recombinant h5β-red for NADPH was determined by measurement of protein fluorescence on a SLM 8000 fluorometer. Measurements were made at 22 °C in a 2 mL cell containing a magnetic stirrer, the purified enzyme (20 mg/mL) and PBS buffer in a final volume of 1 mL. Protein fluorescence was measured following the incremental addition of NADPH (0−5 μM). The total volume change was less than 0.5%. Excitation of samples was at 290 nm with fluorescence emission scanned from 300 to 500 nm at 120 nm/min. Emission and excitation bandpasses were both set to 4 nm. Data were plotted as the percentage change in fluorescence at emission λ_{max} (%Δfluorescence) versus NADPH concentration. K_d values were estimated by fitting these data to a saturation absorption isotherm using the GraphPad Prism program.

Crystallization and X-Ray Analysis of the Recombinant h5β-Reductase. Prior to crystallization, a 4-fold molar ratio of NADPH was added to the concentrated and highly purified h5β-red protein. For h5β-red/NADPH/Δ4 complex, Δ4 was added at a 4-fold molar ratio. Crystals were obtained at 4 °C using the hanging-drop vapor diffusion technique. h5β-Reductase crystals were generally obtained in drops of a 2:1 (v/v) ratio of protein and well solution (see Table 2 for

Table 2: Summary of the Crystallization Conditions

	h5β-reductase in complex with NADPH	h5β-reductase in complex with $NADP^+$ and androst-4-ene-3,20-dione
protein concentration (mg/mL)	12.8	9.55
crystallization temperature (K)	277	277
composition of mother liquor	PEG-4K 20%, 0.1 M Tris, pH 7.5, MPD 5%	PEG-4K 20%, 0.1 M Tris, pH 7.7, MPD 5%, 0.05 M $CaCl_2$
ratio of protein to mother liquor in the drop	2/1	2/1
largest crystal size (mm^3)	0.6 × 0.2 × 0.2	0.6 × 0.2 × 0.2
time to reach the maximum size (days)	5	5
cryoprotecting agent and final concentration used (%)	ethylene glycol 20%	ethylene glycol 20% + 1 mM and rost-4-ene-3,20-dione

crystallization conditions). Crystals appeared rapidly and grew to a suitable size for X-ray diffraction in about 5 days. Prior to diffraction, crystals of h5β-red/NADPH/Δ4 complex were soaked for 5 min in a cryopreservative solution containing 1 mM Δ4 in order to achieve a full occupancy of the steroid-binding site. X-ray diffraction images were recorded at 100 K using our laboratory R-AXIS IIc image-plate detector mounted on a RU-200 copper rotating anode generator equipped with focusing mirrors. Data were integrated and scaled using the XDS program (*25*). The h5β-red structure was obtained by the molecular replacement method with the MOLREP software from CCP4 suite (*26*) using coordinates of the m17α-HSD/NADPH binary complex (2HEJ) (*24*) as a search model. The refinement procedure was performed using Refmac (*27*) and CNS (*28*) programs. The initial model issued from rigid body refinement was manually mutated to match the h5β-reductase sequence and was submitted to a cycle of simulated annealing at 3000 K followed by energy minimization cycles. After electronic density map calculations and manual rebuilding using O (*29*), NADPH cofactor and steroid were added to the model. Models were refined by simple energy minimization followed by isotropic B-factor refinement (restrained, individual B-factor refinement) and corrected by manual rebuilding. Missing parts of the models, β-mercaptoethanol, ethylene glycol, and water molecules were progressively added during the refinement procedure. Finally, the quality of the model was verified with PROCHECK (*30*).

Site-Directed Mutagenesis. Plasmid pGEX-6P1-5β-red Y132F and V309F mutations were performed using the QuickChange site-directed mutagenesis kit (Stratagene) with 5′-GCC-AGG-AGA-TGA-AAT-AT**T**-CCC-TAG-AGA-TGA-GAA-TGG-3′ and 5′-GAA-TAA-AAA-TGT-CCG-CTT-T**T**T-TGA-ATT-GCT-CAT-GTG-GCG-CG-3′ (mutated nucleotides are bold) as forward primers, respectively. Positive clones were sequenced to confirm the presence of the desired mutation.

RESULTS AND DISCUSSION

Characterization of Enzymatic Activity. Since certain steroid metabolizing enzymes of the AKR gene superfamily are labile and lose their activity upon cell homogenization (*31, 32*), we first determine whether our purified h5β-red enzyme preparation had retained its activity toward steroid substrates. Kinetic studies were conducted immediately (or a few days later to test the stability of the recombinant enzyme) after the purification of the enzyme by varying initial concentrations of Δ4 and Prog in the presence of saturating concentrations of NADPH. We found that our highly purified recombinant h5β-red preparation efficiently transforms Δ4 and Prog into 5β-androstanedione and 5β-dihydroprogesterone, respectively, and remains active several days after its purification without marked loss of activity.

We noticed that the h5β-red displays a strong substrate inhibition at relatively low steroid concentrations. Indeed, as seen in Figure 1A, at lower concentrations (up to 0.6 μM of Δ4), the kinetic data fit very well with the Michaelis−Menten equation ($K_m = 0.366 \pm 0.094$ μM and a turnover of 0.78 min^{-1}). However, at higher Δ4 concentrations, the velocity of the enzyme tends to decrease, indicating a substrate inhibition (Figure 1B). The passage from linear Michaelis−Menten behavior to substrate inhibition occurs in a transition zone of Δ4 concentrations ranging from 0.6 to 1.0 μM. Similar substrate inhibition of the enzyme was also observed with Prog (results not shown). Interestingly, it has been previously reported that h5β-red activity can also be reduced or inhibited by an excess of mineralocorticoid (*22*). Thus, patients with mutations affecting the activity of 11β-hydroxysteroid dehydrogenase type 2, the enzyme converting cortisol to cortisone, also have reduced serum and urine levels of 5β-cortisol metabolites, suggesting that cortisol or cortisol metabolites are responsible for inhibition of h5β-red. Human 5β-red is not the only AKR enzyme for which substrate inhibition phenomena have been reported. Indeed, the AKR1C2 enzyme has been found to be substrate-inhibited by the synthetic compound tibolone, while the AKR1C1 enzyme is inhibited by two structurally similar xenobiotic substrates, *E*- and *Z*-10-oxonortriptyline (*33, 34*). However, h5β-red is, to our knowledge, the only AKR enzyme for which substrate inhibition occurs with endogenous ligand. A low level of circulating steroids is probably not sufficient to inhibit h5β-red, but under certain circumstance, like the one described by intracrinology (*35*), the steroid concentrations can potentially be high enough to inhibit the enzyme.

The fact that h5β-red is inhibited by its steroid substrates Δ4 and Prog explains the previously reported contradictory results concerning the activity of this enzyme toward C19- and C21-steroids. Using transiently transfected COS cell homogenates, Kondo et al. (*17*) first reported that h5β-red could not metabolize Δ4 and Prog. Subsequently, Charbonneau and Luu-The (*7*) found that the same enzyme expressed in stably transfected embryonic kidney (HEK-293) cells and assayed in intact cells efficiently catalyzes the 5β-reduction of progestins and androgen hormones, including Prog, 17α-hydroxyprogesterone, Δ4, and Testo. At that time, it was hypothesized that the difference in the experimental conditions used by the two groups (assay of the 5β-red activity in cell homogenates vs intact cells) probably explained the

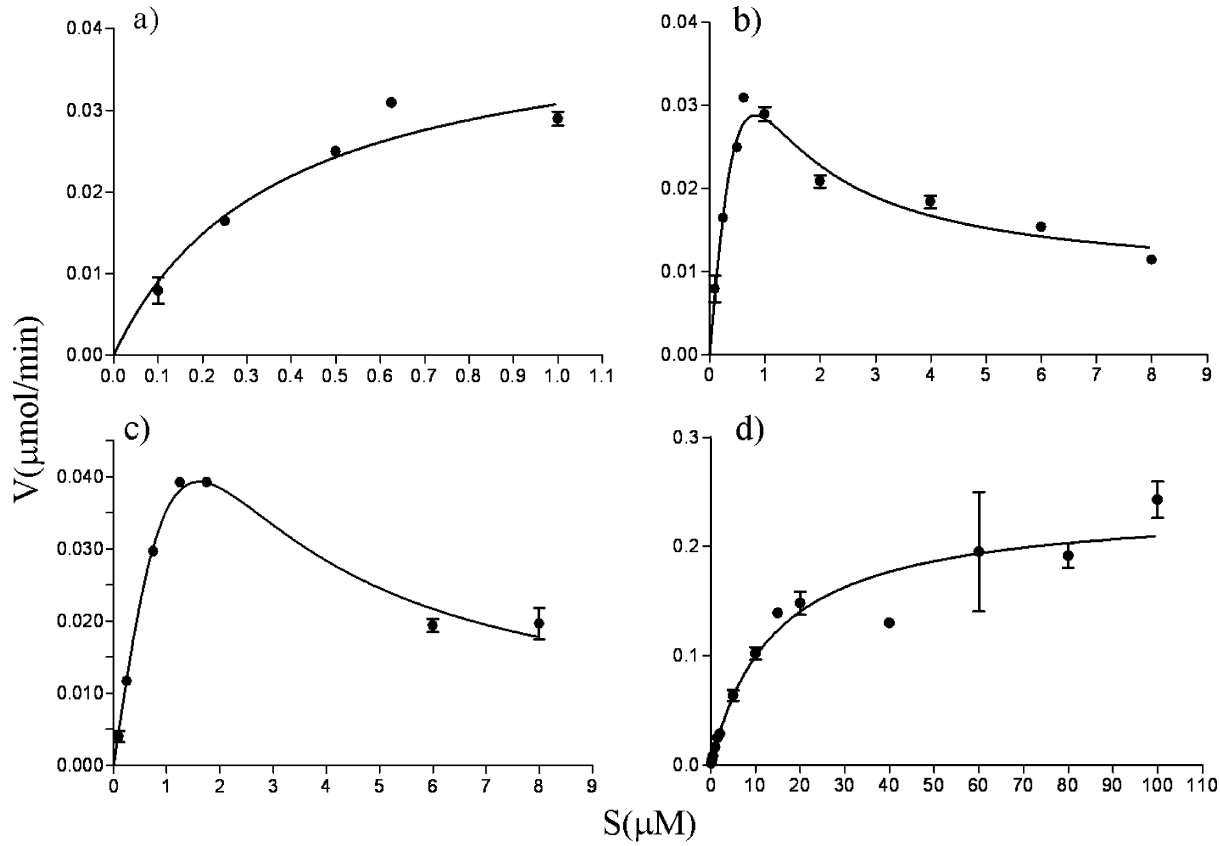

FIGURE 1: Michaelis−Menten kinetics for the reduction of androstenedione by (a) wild-type 5β-red at low substrate concentrations, (b) wild-type 5β-red at higher substrate concentrations, (c) 5β-red(Y132F) mutant, and (d) 5β-red(V309F) mutant. Each point represents the mean of duplicates. Curves in panels a and d are fitted using the Michaelis−Menten equation, while curves in panels b and c are fitted to a substrate inhibition equation.

discrepancy between these two results (*7*). This hypothesis cannot be ruled out; however, our findings about the stability of the recombinant h5β-red upon cell homogenization and, more importantly, the fact that the activity of this enzyme is strongly reduced in the presence of relatively low concentrations of its steroid substrates urged us to re-evaluate the question. Considering that in their activity assays Kondo et al. (*17*) used a steroid concentration (50 μM) that is sufficient to inhibit h5β-red (see above), it is very likely that the amount of 5β-reduced steroids produced in this condition was too low to be easily detected using HPLC techniques. On the other hand, because they used very low steroid substrate concentrations (less than 0.1 μM) coupled with a more sensitive method for the detection of the steroidal products, Charbonneau and Luu-The (*7*) have successfully observed the reductive activity of the h5β-red toward the sexual steroids that have a C4−C5 double bond in their structure.

Finally, we used a protein fluorescence quenching assay to determine the dissociation constant (K_d) for the h5β-red-NADPH complex in order to compare it with those previously measured for two other AKR enzymes, h3α-HSD3 (AKR1C2) and m17α-HSD (AKR1C21) (Table 1). As previously demonstrated (*23*), the number of hydrophilic interactions forming the well-known "safety belt" of AKR enzymes directly affects the binding of the cofactor. We have shown that higher the K_d, tighter is the safety belt, because of the increased number of H-bonds maintaining the two loops forming the safety belt in a closed conformation. On the other hand, low K_d means fewer interactions favoring the two loops to be in an open conformation. In the open conformation, AKR enzymes are more prone to bind NADPH but also are more prone to expel the oxidized $NADP^+$. The high K_d value directly indicates a better stabilization of the safety belt in the closed conformation, and the enzyme needs a higher cofactor concentration to bind. Once bound to a high K_d AKR, the cofactor is trapped in the active site, and the tighter safety belt is less prone to open again and to release the cofactor. We thus found that the K_d for binding of NADPH by h5β-red (528 ± 28 nM) is very similar to that of m17α-HSD (459 ± 24 nM) but more than 5-fold lower than that determined for h3α-HSD3 (2702 ± 140 nM) by the same method. This indicates that NADPH binding is easier in h5β-red than in h3α-HSD3 and at a comparable level to that in m17α-HSD. This is in perfect agreement with the fact that binary complex crystals have been easily obtained for h3α-HSD3 without the need to add cofactor during the purification and crystallization processes, whereas addition of NADPH is absolutely required to obtain such binary complex crystals for h5β-red and m17α-HSD enzymes (*24, 36, 37*).

Crystallization of h5β-Reductase in Complex with NADPH. In order to better understand the peculiarities of h5β-red in terms of cofactor binding and stabilization, we crystallized this enzyme in the presence of NADPH and compared it to other AKR1C enzyme binary complexes. Human 5β-red crystals obtained in the presence of NADPH were used for X-ray diffraction experiments, and a near complete data set was collected to 2.2 Å resolution (see Table 2 for crystallization conditions and Table 3 for data collection and refinement statistics). The h5β-red structure adopts the

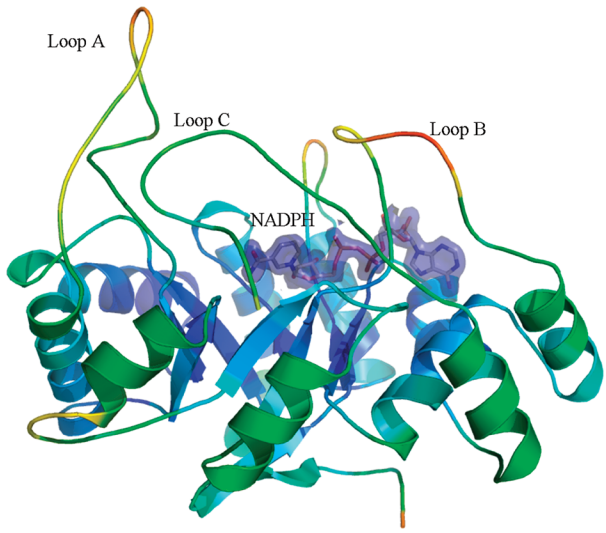

FIGURE 2: Overall view of h5β-reductase in binary complex with NADPH. The ribbon representation shows the three mobile loops (loops A, B, and C), all of which are located at the C-terminal end of the β-barrel and which contribute to forming the cofactor and steroid binding sites. $2F_o - F_c$ electronic density map of NADPH is contoured at 1σ level. Protein structure is colored according to B-factor (from dark blue for low B-factor to red for high B-factor). The figure was generated with Pymol (Delano Scientific).

conserved TIM barrel fold and a very clear electronic density was observed for the NADPH molecule in each monomer (see Figure 2). Our h5β-red binary complex model was refined to an *R*-factor of 21.6% (R_{free} = 25.1%). The three additional residues of h5β-red (Leu_3, Pro_{11}, and Lys_{30}) were unambiguously fit in the $F_o - F_c$ electronic map. However, for Lys_{30} electron density was only present for the backbone atoms. In addition, the first residue of each monomer (Met_1) was not modeled, since no electron density was observed. Finally, a water molecule was found in the catalytic site of both monomers, in a position that could correspond to that of the O3 atom found in all steroid and bile acid substrates of this enzyme. This water molecule is indeed hydrogen-bonded to Tyr_{58} and Glu_{120}, two residues of the catalytic tetrad. Finally, a MPD molecule originating from the crystallization was found in the ligand binding pocket of monomer A.

Binding of the Cofactor by h5β-Reductase and Identification of the Safety Belt Interactions. Binding of the cofactor molecule constitutes the first step of the sequential ordered Bi−Bi mechanism characterizing enzymes of the AKR superfamily (*38, 39*). The NADPH molecule binds at the C-terminal end of the β-barrel (see Figure 2) and interacts with many hydrophilic residues distributed all along the cofactor molecule. A close examination of the hydrogen bond network established by h5β-red with the NADPH molecule in our binary complex structure has allowed us to identify 18 putative H-bonds involving 16 amino acid residues. This hydrogen bond network is essentially the same as the one observed in the h3α-HSD3 binary complex (*24*), in which we have identified a total of 19 hydrogen bonds formed by 16 residues. Moreover, there is no major difference in the nature of the amino acid residues involved in cofactor binding between these two enzymes nor in the distance separating the atoms making these interactions. It is thus very likely that other structural factors exist that can explain the difference in cofactor binding affinity measured for h5β-red and h3α-HSD3.

Binding of the cofactor induces a large structural rearrangement of loop B over the NADPH molecule, providing additional interactions, especially with the central phosphate groups (*24*). Furthermore, in this new conformation, loop B residues are able to establish other strong hydrophilic interactions with residues of a small loop β1−α1 located on the opposite side of the cofactor binding cleft. In this particular position over the cofactor, loop B acts as a "safety belt" (*40*) and contributes to the maintenance of the cofactor tightly bound to the enzyme. By comparing the structure of different AKR enzymes in binary complex with NADPH and by proceeding to site-directed mutagenesis experiments, we have recently shown that the number and strength of the hydrogen bonds involved the safety belt could be directly related to the binding constant of NADPH, even if no residue of the safety belt makes any direct interaction with the cofactor (*23, 24, 41*). Briefly, the weaker the stabilization of the two loops of the safety belt, the lower is the binding constant. If the loops are less stabilized as observed in m17α-HSD, they are more prone to be in an open conformation and to facilitate the NADPH binding (or release of the product). On the other hand, a strong network of H-bonds in the safety belt, as observed for h3α-HSD3, can impede the binding of NADPH or the release of the oxidized product. In the h5β-red binary complex structure reported here, there is only one hydrogen bond at the interface of loop B and loop β1−α1 (between residues Glu_{28} and Asn_{227}), a quite similar structural arrangement to that found in the m17α-HSD structure but one that differs from that observed in the h3α-HSD3 structure (Figure 3A−C). Interestingly, this finding is again in perfect agreement with the K_d values determined for these three enzyme−NADPH complexes (Table 1). On the other hand, the position of the single hydrogen bond joining loop B and loop β1−α1 in h5β-red (Figure 3A) differs from that found in the m17α-HSD safety belt (Figure 3C). Indeed, in the h5β-red safety belt, the interloop hydrogen bond is located near the top extremity of the loops, while it is located at the bottom portion in the m17α-HSD structure. The main structural consequence of this difference is that the two loops are slightly more distant from each other in h5β-red compared with m17α-HSD or h3α-HSD (Figure 3D). As a result, the steroid-binding cavity of h5β-red is substantially larger than that of the two other enzymes (Figure 3A−C, right panels).

Crystallization of h5β-Reductase in the Presence of NADPH and Androstenedione and Overall Description of the Structure. As mentioned above, h5β-red demonstrates a strong substrate inhibition in the presence of low concentrations of Δ4. We characterized, at the molecular level, this inhibition mechanism by determining the crystal structure of h5β-red in the presence of Δ4. Ternary complex crystals of h5β-red were obtained by adding a 4-fold molar excess of Δ4 to the concentrated protein prior to its crystallization (see Table 2 for crystallization conditions). The near complete data set (see Table 3 for data collection and refinement statistics) allowed us to build a model with two protein molecules per asymmetric unit at 2.0 Å resolution. The cofactor molecules (one for each monomer) were unambiguously fit in the electronic density. We also found a large electronic density that corresponded very well to the shape

Table 3: Summary of Data Collection and Refinement Statistics

	h5β-reductase in complex with NADPH	h5β-reductase in complex with $NADP^+$ and androst-4-ene-dione
Data Collection		
resolution (Å)	19.7−2.2 (2.3−2.2)	19.6−2.0 (2.1−2.0)
unit cell params		
a, *b*, *c* (Å)	50.38, 110.63, 130.65	50.41, 110.87, 130.28
α, β, γ (deg)	90	90
space group	$P2_12_12_1$	$P2_12_12_1$
total reflns	132357 (15704)	384886 (21805)
unique reflns	36835 (4411)	47996 (5657)
completeness (%)	97.2 (95)	95.6 (83.8)
$I/\sigma I$	16.2 (4.8)	21.3 (5.1)
R_{merge} (%)	10.2 (28.1)	7.4 (23.3)
redundancy	3.6 (3.6)	8.0 (3.9)
Refinement		
reflns used, *R* work set/R_{free} set	35278/1854	45704/2435
R_{cryst} (%)	21.6	20.8
R_{free} (%)	25.1	23.8
rmsd from ideal, bondlength (Å)/angle (deg)	0.007/1.2	0.007/1.2
non-hydrogen atoms		
all atoms	5693	5923
protein	5283	5296
NADPH	96	96
steroids	N/A	42
water	278	461
heterogeneous atoms	36	28
overall B factors (Å^2)	21.1	14.0
cofactor B factors (Å^2)	17.8	10.4
steroids B factors (Å^2)	N/A	23.5
Verification with PROCHECK (%)		
most favored regions	88.8	89.7
allowed regions	12.2	10
disallowed regions	0	0.3

of an all-*trans* steroid skeleton, suggesting that the steroid bound to the enzyme had not been 5β-reduced. After close examination, we found that the bound steroid very likely corresponded to the Δ4 added to the protein at the moment of its crystallization. However, the Δ4 molecule was not profoundly inserted into the steroid-binding cavity with its A ring toward the catalytic site in a position allowing its 5β-reduction. It was instead positioned at the entry of the cavity, firmly tethered by hydrogen bonds at both its extremities (Figure 4). Indeed, the C3-keto oxygen atom of Δ4 established strong hydrogen bonds with the side chain of Ser_{225} and backbone of Asn_{227}, two residues belonging to loop B, while its C17-keto oxygen atom was H-bonded to the hydroxyl group of Tyr_{132} residue. In addition, the steroid nucleus was also very well stabilized by hydrophobic interactions involving Val_{309} and Trp_{230}, whose indole ring side chains were perfectly stacked against rings C and D. In this position and orientation, the bound Δ4 obviously hinders access to the catalytic site of the h5β-red enzyme for the incoming steroid substrates. It also prevents a substrate molecule from binding h5β-red in a catalytically productive position (Figure 5). Finally, because its stabilization in this subsite involves the Asn_{227} residue of loop B, Δ4 also certainly interferes with the formation or the opening of the safety belt and, consequently, with the binding or release of the cofactor.

In addition to the obstruction created by the steroid bound in this alternative position, the Trp_{230} side chain also contributes to diminishing the size of the opening of the steroid-binding cavity. In the 5β-red/NADPH binary complex structure, the indole ring of Trp_{230} is turned approximately 90° and is positioned in the space occupied by the steroid A-ring in the h5β-red/NADPH/Δ4 ternary complex structure (Figure 6). This suggests that Trp_{230} acts as a swinging door, controlling the passage of steroid substrates toward the catalytic site of h5β-red. Thus, in the binary complex, the side chain of Trp_{230} has sufficient space to flip and to clear the opening of the steroid-binding cavity, allowing the passage of a steroid molecule toward the catalytic site of the enzyme. However, when a steroid molecule is bound in the alternative binding site, Trp_{230} can no longer flip or rotate, contributing to a barrier able to efficiently impede any other steroid molecules from reaching the active site of h5β-red. It is thus more than likely that this subsite, or alternative binding site, within the substrate-binding site where the Δ4 molecule is bound in the present ternary complex structure corresponds to the inhibitor-binding site responsible for the competitive substrate inhibition phenomenon observed.

Characterization of the Alternative Binding Site of h5β-Reductase. We used site-directed mutagenesis to verify this hypothesis and to better characterize this alternative steroid-binding site in order to determine its importance in the mechanism of substrate inhibition of h5β-red. We first mutated residues directly involved in Δ4 stabilization in the alternative binding site. At the O3 extremity, the replacement of Asn_{227} was useless since this residue establishes a hydrogen bond with Δ4 via its backbone amino group (-NH). Consequently, it was impossible to completely eliminate the interaction made by the enzyme with this part of the steroid, even when removing the other hydrogen bond made by the Ser_{225} residue. We instead mutate the residue that maintains the other extremity of Δ4 (O17 atom), Tyr_{132}, and change it

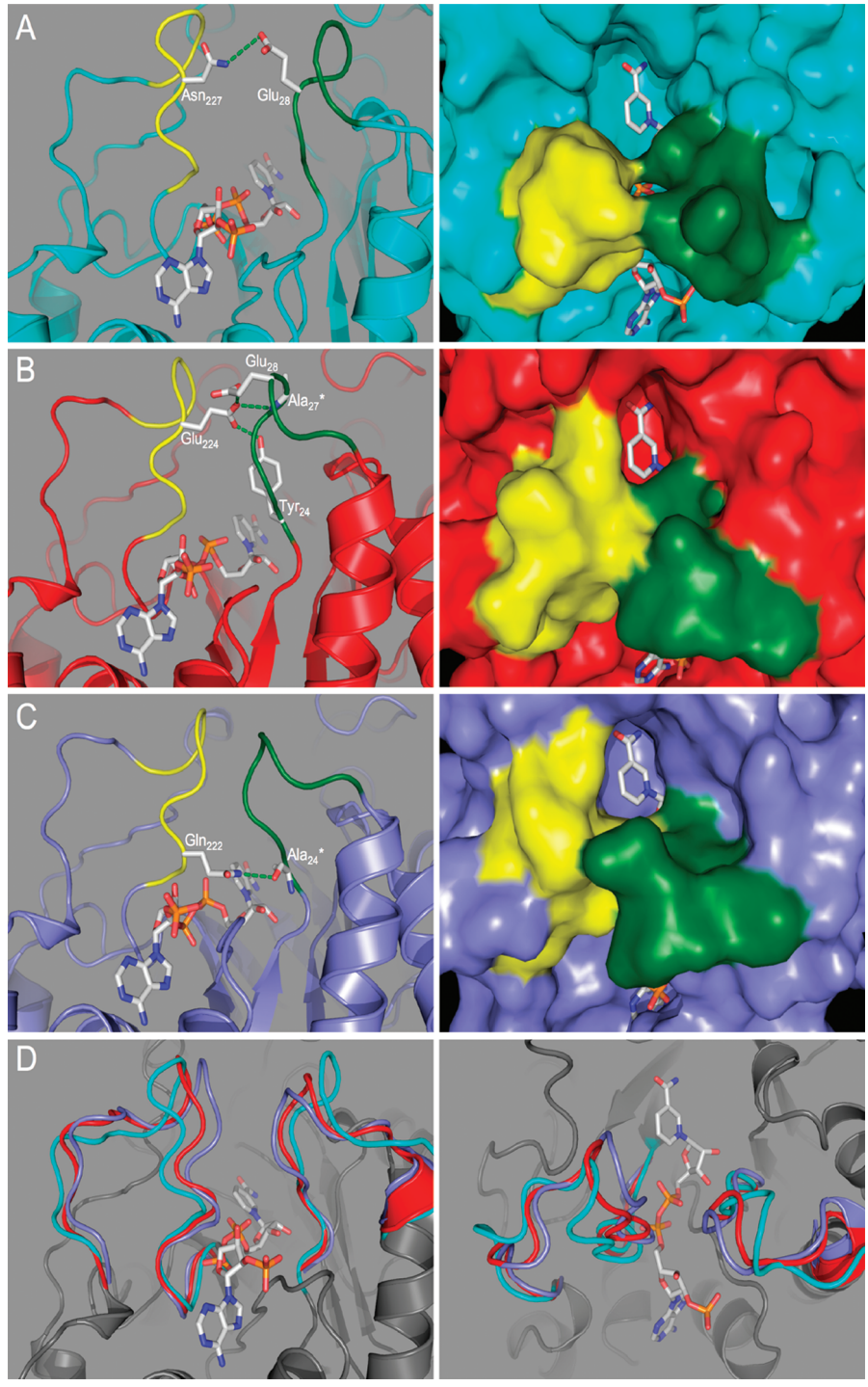

FIGURE 3: Comparison of the "safety belt" formation following NADPH binding in (A) h5β-reductase-NADPH, (B) human type 3 3α-HSD-NADPH, and (C) mouse 17α-HSD-NADPH binary complexes (left panels). For simplification, only residues involved in the formation of hydrogen bonds (dashed green lines) connecting the mobile loop B and the small β1−α1 loop are depicted. Asterisks (*) indicate that the interaction is with the main chain. The impact of the position of the mobile loop B (in yellow) and the small β1−α1 loop (in green) on the shape and size of the enzyme's steroid-binding cavity is also shown (right panels). Panels D show two orthogonal views of a superimposition of the three safety belts: h5β-red in cyan, h3α-HSD3 in red, and m17α-HSD in purple. The figure was generated with Swiss-PDB viewer (*45*) and Pymol (Delano Scientific).

to a phenylalanine, a residue frequently found at this position in the structure of many other AKR enzymes. Astonishingly, kinetic assays showed that the h5β-red($Y_{132}F$) mutant enzyme was still substrate-inhibited by Δ4, albeit the transition zone of Δ4 concentrations at which the substrate inhibition phenomenon occurs was slightly shifted, now ranging from 1.0 to 2.0 μM (Figure 1C). The catalytic efficiency of the mutated enzyme was also similar to that of the wild-type h5β-red enzyme (Table 4). Consequently, if the alternative binding site identified in the h5β-red/NADPH/Δ4 ternary complex structure really corresponds to the inhibitor-binding site, this result indicates that the loss of the interaction between Tyr132 and the O17 atom of Δ4 has a very limited impact on the binding of the steroid substrates to this site.

Following this unsuccessful attempt to diminish the affinity of Δ4 for the alternative binding site, we increased steric

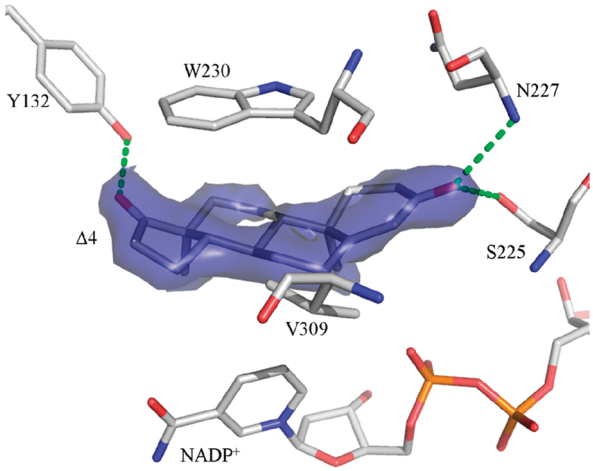

FIGURE 4: Close-up view of residues interacting with the androstenedione (Δ4) molecule in the alternative binding site of monomer A. The figure shows residues making H-bonds (dashed green lines) with Δ4, namely, Tyr_{132}, Ser_{225}, and Asn_{227}. Residues making hydrophobic contacts with the steroid, namely, Trp_{230} and Val_{309}, are also represented. The $2F_o - F_c$ map for Δ4 is contoured at 1σ level. Atoms are colored using standard CPK color set, and the figure was generated with PyMol (Delano Scientific).

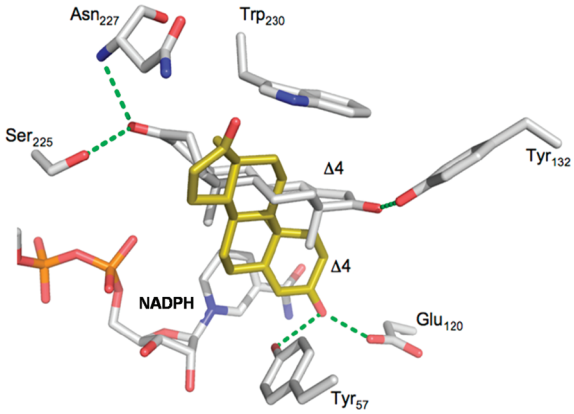

FIGURE 5: View of the two mutually exclusive positions for a Δ4 molecule in the steroid-binding site of h5β-red. The figure shows Δ4 bound in a productive or catalytic orientation (in gold) and in a nonproductive orientation (in standard CPK color set). Residues making H-bonds (dashed green lines) with Δ4 when bound in the alternative site (Tyr_{132}, Ser_{225}, and Asn_{227}) or in the catalytic site (Tyr_{57} and Glu_{120}) are also represented. The figure was generated with PyMol (Delano Scientific).

hindrance directly inside the alternative binding site in order to more drastically disturb the enzyme−Δ4 interaction. As observed in Figure 6, when Δ4 occupies the alternative binding site, the Val_{309} side chain makes a hydrophobic contact with the steroid nucleus around its C6 and C7 atoms. By replacing this small residue with a bulky phenylalanine, we made the h5β-red enzyme unable to bind Δ4 in the alternative position. This was confirmed by kinetic assays made on the h5β-red(V_{309}F) mutant enzyme, which showed that the enzyme is no longer inhibited by the substrate, even at high Δ4 concentrations (Figure 1D). It thus appears that the Δ4 substrate now has free access to the catalytic site of h5β-red(V_{309}F), since the mutation has made its high-affinity alternative steroid-binding site inaccessible. However, h5β-red(V_{309}F) displays a 13.6-fold reduced catalytic efficacy compared with the wild-type enzyme, probably because the steric hindrance generated by the presence of a phenylalanine residue at position 309 also restrains the capacity of the side

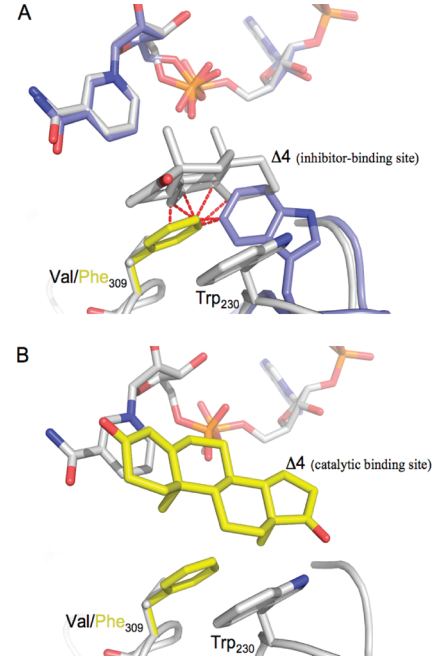

FIGURE 6: Likely impact of the replacement of the valine residue at position 309 by a phenylalanine on the binding of a Δ4 molecule in the steroid-binding site of h5β-red. (A) The presence of a bulky side chain at position 309 very likely impedes (indicated by red broken lines) both binding of Δ4 in the inhibitor-binding site (in standard CPK color set) and Trp_{230} from occupying the position observed in the binary complex structure (in blue). (B) On the other hand, it seems that the Val_{309}Phe mutation always allows the passage of a Δ4 molecule (in gold) into the active site of h5β-red and its binding in a productive or catalytic orientation. The figure was generated with PyMol (Delano Scientific).

Table 4: Steady-State Kinetic Parameters for Androstenedione Reduction Catalyzed by the Wild-Type and Mutated Forms of h5β-Reductase

enzyme	K_m (μM)	K_{cat} (min^{-1})	K_{cat}/K_m (min^{-1} μM^{-1})
h5β-reductase	0.366 ± 0.094	0.78	2.13
h5β-red(Y132F)	0.974 ± 0.22	2.43	2.49
h5β-red(V309F)	16.29 ± 2.12	2.55	0.156

chain of the Trp_{230} residue to flip and to completely clear the passage toward the catalytic site of the enzyme. This is supported by the fact that Val_{309} and Trp_{230} residues are in close proximity. It is likely that the phenyl ring of the Phe_{309} fills the space occupied by the ring B of Δ4 bound in the alternative binding site and can therefore interfere with the indole ring of the Trp_{230} residue (Figure 6A). In addition, in this position the bulky side chain of Phe_{309} considerably reduces the size of the steroid binding cavity, explaining why the K_m value of h5β-red(V_{309}F) for Δ4 (Table 4) is significantly increased (44.5-fold over that of the wild-type enzyme). Indeed, in the manual docking experiments we have made for this enzyme (see above), the side chain of a phenylalanine residue placed at this position pointed inside the steroid binding cavity and interacted very closely with the angular methyl groups (C18 and C19 atoms) of a Δ4 molecule positioned in the catalytic site in an optimal position for its 5β-reduction (Figure 6B). Nevertheless, considering the plasticity of residues delineating the steroid-binding site, a well-known characteristic of the AKR enzyme family (*42, 43*), it is also possible that the position of other residues is affected by the presence of Phe_{309}, therefore also potentially contrib-

uting to the change in substrate affinity observed in the mutant enzyme.

Concluding Remarks. During the review of this work, crystal structures of the human 5β-red in complex with various substrates have been published by another group. Similar to the result discussed here, Di Costanzo et al. (*44*) published a structure of h5β-red in complex with testosterone in the same alternative binding site we have identified. It is noteworthy that the coordinates of our structures were deposited to the RCSB PDB before the published structure of Di Costanzo et al. (*44*). In addition, these authors did not characterize this subsite by performing site-directed mutations or kinetic assays. The interactions made by the testosterone molecule observed in their complex are identical to what we observed for Δ4. Furthermore, contrary to the published structures by Di Costanzo et al., we have identified a structural rearrangement of Trp_{230} between our h5β-red/NADPH and h5β-red/NADPH/Δ4 complexes. The presence of a glycerol molecule in the vicinity of Trp_{230} of the Di Costanzo et al. (*44*) binary complex certainly impedes this residue from adopting the conformation we have identified in our binary complex. We have suggested that this residue can act as a swinging door to allow the steroid to enter in the active site or in the substrate inhibition site depending upon its conformation.

ACKNOWLEDGMENT

The authors thank Penny Soucy and Samantha Jennie Hyde for careful reading of manuscript.

REFERENCES

1. Berseus, O. (1967) Conversion of cholesterol to bile acids in rat: Purification and properties of a delta-4-3-ketosteroid 5-beta-reductase and a 3-alpha-hydroxysteroid dehydrogenase. *Eur. J. Biochem. 2*, 493–502.
2. Berseus, O., and Bjorkhem, L. (1967) Enzymatic conversion of a delta-4-3-ketosteroid into a 3-alpha-hydroxy-5-beta steroid: Mechanism and stereochemistry of hydrogen transfer from NADPH. Bile acids and steroids 190. *Eur. J. Biochem. 2*, 503–507.
3. Berseus, O., Danielsson, H., and Kallner, A. (1965) Synthesis and metabolism of cholest-4-ene-7-alpha,12-alpha-diol-3-one and 5-beta-cholestane-7-alpha,12-alpha-diol-3-one. Bile acids and steroids 153. *J. Biol. Chem. 240*, 2396–2401.
4. Clayton, P. T., Patel, E., Lawson, A. M., Carruthers, R. A., Tanner, M. S., Strandvik, B., Egestad, B., and Sjovall, J. (1988) 3-Oxo-delta 4 bile acids in liver disease. *Lancet 1*, 1283–1284.
5. Lemonde, H. A., Custard, E. J., Bouquet, J., Duran, M., Overmars, H., Scambler, P. J., and Clayton, P. T. (2003) Mutations in SRD5B1 (AKR1D1), the gene encoding delta(4)-3-oxosteroid 5beta-reductase, in hepatitis and liver failure in infancy. *Gut 52*, 1494–1499.
6. Setchell, K. D., Suchy, F. J., Welsh, M. B., Zimmer-Nechemias, L., Heubi, J., and Balistreri, W. F. (1988) Delta 4-3-oxosteroid 5 beta-reductase deficiency described in identical twins with neonatal hepatitis. A new inborn error in bile acid synthesis. *J. Clin. Invest. 82*, 2148–2157.
7. Charbonneau, A., and The, V. L. (2001) Genomic organization of a human 5beta-reductase and its pseudogene and substrate selectivity of the expressed enzyme. *Biochim. Biophys. Acta 1517*, 228–235.
8. Okuda, A., and Okuda, K. (1984) Purification and characterization of delta 4-3-ketosteroid 5 beta-reductase. *J. Biol. Chem. 259*, 7519–7524.
9. Bertilsson, G., Heidrich, J., Svensson, K., Asman, M., Jendeberg, L., Sydow-Backman, M., Ohlsson, R., Postlind, H., Blomquist, P., and Berkenstam, A. (1998) Identification of a human nuclear receptor defines a new signaling pathway for CYP3A induction. *Proc. Natl. Acad. Sci. U.S.A. 95*, 12208–12213.
10. Granick, S., and Kappas, A. (1967) Steroid control of porphyrin and heme biosynthesis: a new biological function of steroid hormone metabolites. *Proc. Natl. Acad. Sci. U.S.A. 57*, 1463–1467.
11. Kappas, A., and Granick, S. (1968) Experimental hepatic porphyria: Studies with steroids of physiological origin in man. *Ann. N.Y. Acad. Sci. 151*, 842–849.
12. Levere, R. D., and Granick, S. (1965) Control of hemoglobin synthesis in the cultured chick blastoderm by delta-aminolevulinic acid synthetase: Increase in the rate of hemoglobin formation with delta-aminolevulinic acid. *Proc. Natl. Acad. Sci. U.S.A. 54*, 134–137.
13. Levere, R. D., Kappas, A., and Granick, S. (1967) Stimulation of hemoglobin synthesis in chick blastoderms by certain 5beta androstane and 5beta pregnane steroids. *Proc. Natl. Acad. Sci. U.S.A. 58*, 985–990.
14. Moore, L. B., Parks, D. J., Jones, S. A., Bledsoe, R. K., Consler, T. G., Stimmel, J. B., Goodwin, B., Liddle, C., Blanchard, S. G., Willson, T. M., Collins, J. L., and Kliewer, S. A. (2000) Orphan nuclear receptors constitutive androstane receptor and pregnane X receptor share xenobiotic and steroid ligands. *J. Biol. Chem. 275*, 15122–15127.
15. Kubli-Garfias, C., Medrano-Conde, L., Beyer, C., and Bondani, A. (1979) In vitro inhibition of rat uterine contractility induced by 5 alpha and 5 beta progestins. *Steroids 34*, 609–617.
16. Sheehan, P. M., Rice, G. E., Moses, E. K., and Brennecke, S. P. (2005) 5 Beta-dihydroprogesterone and steroid 5 beta-reductase decrease in association with human parturition at term. *Mol. Hum. Reprod. 11*, 495–501.
17. Kondo, K. H., Kai, M. H., Setoguchi, Y., Eggertsen, G., Sjoblom, P., Setoguchi, T., Okuda, K. I., and Bjorkhem, I. (1994) Cloning and expression of cDNA of human delta 4-3-oxosteroid 5 beta-reductase and substrate specificity of the expressed enzyme. *Eur. J. Biochem. 219*, 357–363.
18. Onishi, Y., Noshiro, M., Shimosato, T., and Okuda, K. (1991) Molecular cloning and sequence analysis of cDNA encoding delta 4-3-ketosteroid 5 beta-reductase of rat liver. *FEBS Lett. 283*, 215–218.
19. Charbonneau, A., and Luu-The, V. (1999) Assignment of steroid 5beta-reductase (SRD5B1) and its pseudogene (SRD5BP1) to human chromosome bands 7q32→q33 and 1q23→q25, respectively, by in situ hybridization. *Cytogenet. Cell Genet. 84*, 105–106.
20. Faucher, F., Cantin, L., Luu-The, V., Labrie, F., and Breton, R. (2008) The crystal structure of human Delta4-3-ketosteroid 5beta-reductase defines the functional role of the residues of the catalytic tetrad in the steroid double bond reduction mechanism. *Biochemistry 47*, 8261–8270.
21. Jez, J. M., and Penning, T. M. (1998) Engineering steroid 5 beta-reductase activity into rat liver 3 alpha-hydroxysteroid dehydrogenase. *Biochemistry 37*, 9695–9703.
22. Morineau, G., Marc, J. M., Boudi, A., Galons, H., Gourmelen, M., Corvol, P., Pascoe, L., and Fiet, J. (1999) Genetic, biochemical, and clinical studies of patients with A328V or R213C mutations in 11betaHSD2 causing apparent mineralocorticoid excess. *Hypertension 34*, 435–441.
23. Faucher, F., Cantin, L., Pereira de Jesus-Tran, K., Lemieux, M., Luu-The, V., Labrie, F., and Breton, R. (2007) Mouse 17alpha-hydroxysteroid dehydrogenase (AKR1C21) binds steroids differently from other aldo-keto reductases: identification and characterization of amino acid residues critical for substrate binding. *J. Mol. Biol. 369*, 525–540.
24. Faucher, F., Pereira de Jesus-Tran, K., Cantin, L., Luu-The, V., Labrie, F., and Breton, R. (2006) Crystal structures of mouse 17alpha-hydroxysteroid dehydrogenase (apoenzyme and enzyme-NADP(H) binary complex): identification of molecular determinants responsible for the unique 17alpha-reductive activity of this enzyme. *J. Mol. Biol. 364*, 747–763.
25. Kabsch, W. (1993) Automatic processing of rotation diffraction data from crystals of initially unknown symmetry and cell constants. *J. Appl. Crystallogr. 26*, 795–800.
26. Bailey, S. (1994) The Ccp4 suite - programs for protein crystallography. *Acta Crystallogr. D50*, 760–763.
27. Murshudov, G. N., Vagin, A. A., and Dodson, E. J. (1997) Refinement of macromolecular structures by the maximum-likelihood method. *Acta Crystallogr. D53*, 240–255.
28. Brunger, A. T., Adams, P. D., Clore, G. M., DeLano, W. L., Gros, P., Grosse-Kunstleve, R. W., Jiang, J. S., Kuszewski, J., Nilges, M., Pannu, N. S., Read, R. J., Rice, L. M., Simonson, T., and Warren, G. L. (1998) Crystallography & NMR system: A new

software suite for macromolecular structure determination. *Acta Crystallogr. D54*, 905–921.
29. Jones, T. A., Zou, J. Y., Cowan, S. W., and Kjeldgaard, M. (1991) Improved methods for building protein models in electron-density maps and the location of errors in these models. *Acta Crystallogr. A47*, 110–119.
30. Laskowski, R. A., Macarthur, M. W., Moss, D. S., and Thornton, J. M. (1993) Procheck - a program to check the stereochemical quality of protein structures. *J. Appl. Crystallogr. 26*, 283–291.
31. Dufort, I., Labrie, F., and Luu-The, V. (2001) Human types 1 and 3 3 alpha-hydroxysteroid dehydrogenases: differential lability and tissue distribution. *J. Clin. Endocrinol. Metab. 86*, 841–846.
32. Dufort, I., Rheault, P., Huang, X. F., Soucy, P., and Luu-The, V. (1999) Characteristics of a highly labile human type 5 17beta-hydroxysteroid dehydrogenase. *Endocrinology 140*, 568–574.
33. Breyer-Pfaff, U., and Nill, K. (1999) Stereoselective high-affinity reduction of ketonic nortriptyline metabolites and of ketotifen by aldo-keto reductases from human liver. *Adv. Exp. Med. Biol. 463*, 473–480.
34. Steckelbroeck, S., Jin, Y., Oyesanmi, B., Kloosterboer, H. J., and Penning, T. M. (2004) Tibolone is metabolized by the 3alpha/3beta-hydroxysteroid dehydrogenase activities of the four human isozymes of the aldo-keto reductase 1C subfamily: inversion of stereospecificity with a delta5(10)-3-ketosteroid. *Mol. Pharmacol. 66*, 1702–1711.
35. Labrie, F. (1991) Intracrinology. *Mol. Cell. Endocrinol. 78*, C113−C118.
36. Couture, J. F., de Jesus-Tran, K. P., Roy, A. M., Cantin, L., Cote, P. L., Legrand, P., Luu-The, V., Labrie, F., and Breton, R. (2005) Comparison of crystal structures of human type 3 3alpha-hydroxysteroid dehydrogenase reveals an "induced-fit" mechanism and a conserved basic motif involved in the binding of androgen. *Protein Sci. 14*, 1485–1497.
37. Nahoum, V., Gangloff, A., Legrand, P., Zhu, D. W., Cantin, L., Zhorov, B. S., Luu-The, V., Labrie, F., Breton, R., and Lin, S. X. (2001) Structure of the human 3alpha-hydroxysteroid dehydrogenase type 3 in complex with testosterone and NADP at 1.25-A resolution. *J. Biol. Chem. 276*, 42091–42098.
38. Askonas, L. J., Ricigliano, J. W., and Penning, T. M. (1991) The kinetic mechanism catalysed by homogeneous rat liver 3 alpha-hydroxysteroid dehydrogenase. Evidence for binary and ternary dead-end complexes containing non-steroidal anti-inflammatory drugs. *Biochem. J. 278* (Part 3), 835–841.
39. Cooper, W. C., Jin, Y., and Penning, T. M. (2007) Elucidation of a complete kinetic mechanism for a mammalian hydroxysteroid dehydrogenase (HSD) and identification of all enzyme forms on the reaction coordinate: the example of rat liver 3alpha-HSD (AKR1C9). *J. Biol. Chem. 282*, 33484–33493.
40. Borhani, D. W., Harter, T. M., and Petrash, J. M. (1992) The crystal structure of the aldose reductase.NADPH binary complex. *J. Biol. Chem. 267*, 24841–24847.
41. Couture, J. F., Legrand, P., Cantin, L., Luu-The, V., Labrie, F., and Breton, R. (2003) Human 20alpha-hydroxysteroid dehydrogenase: crystallographic and site-directed mutagenesis studies lead to the identification of an alternative binding site for C21-steroids. *J. Mol. Biol. 331*, 593–604.
42. Couture, J. F., Legrand, P., Cantin, L., Labrie, F., Luu-The, V., and Breton, R. (2004) Loop relaxation, a mechanism that explains the reduced specificity of rabbit 20alpha-hydroxysteroid dehydrogenase, a member of the aldo-keto reductase superfamily. *J. Mol. Biol. 339*, 89–102.
43. Penning, T. M., Burczynski, M. E., Jez, J. M., Hung, C. F., Lin, H. K., Ma, H., Moore, M., Palackal, N., and Ratnam, K. (2000) Human 3alpha-hydroxysteroid dehydrogenase isoforms (AKR1C1-AKR1C4) of the aldo-keto reductase superfamily: functional plasticity and tissue distribution reveals roles in the inactivation and formation of male and female sex hormones. *Biochem. J. 351*, 67–77.
44. Di Costanzo, L., Drury, J. E., Penning, T. M., and Christianson, D. W. (2008) Crystal structure of human liver Delta(4)-3-ketosteroid 5 beta-reductase (AKR1D1) and implications for substrate binding and catalysis. *J. Biol. Chem. 283*, 16830–16839.
45. Guex, N., and Peitsch, M. C. (1997) SWISS-MODEL and the Swiss-PdbViewer: An environment for comparative protein modeling. *Electrophoresis 18*, 2714–2723.

BI801276H